Turn-on fluorescent sensor for the detection of glucose using manganese dioxide–phenol formaldehyde resin nanocomposite

Zhong Feng Gao, Asmerom Yohannes Ogbe, Ei Ei Sann, Xudong Wang, Fan Xia

www.elsevier.com/locate/talanta

PII: S0039-9140(17)31200-6
DOI: https://doi.org/10.1016/j.talanta.2017.11.073
Reference: TAL18135

To appear in: *Talanta*

Received date: 28 August 2017
Revised date: 28 November 2017
Accepted date: 29 November 2017

Cite this article as: Zhong Feng Gao, Asmerom Yohannes Ogbe, Ei Ei Sann, Xudong Wang and Fan Xia, Turn-on fluorescent sensor for the detection of glucose using manganese dioxide–phenol formaldehyde resin nanocomposite, *Talanta,* https://doi.org/10.1016/j.talanta.2017.11.073

Turn-on fluorescent sensor for the detection of glucose using manganese dioxide–phenol formaldehyde resin nanocomposite

Zhong Feng Gao[a,1], Asmerom Yohannes Ogbe [a,1], Ei Ei Sann[a], Xudong Wang[a], Fan Xia[a,b,*]

[a] Hubei Key Laboratory of Bioinorganic Chemistry & Materia Medica, School of Chemistry and Chemical Engineering, Huazhong University of Science and Technology (HUST), 1037 Luoyu Road, Wuhan 430074, China

[b] Faculty of Materials Science and Chemistry, China University of Geosciences, Wuhan 430074, China

*Correspondence to: Fan Xia: Phone number: 027-87543032; E-mail: xiafan@hust.edu.cn

[1]These authors contributed to this work equally.

Abstract

Monitoring blood glucose has attracted considerable attention because diabetes mellitus is a global public health problem. Herein, we reported a turn-on fluorescence detection strategy based on manganese dioxide (MnO_2)-phenol formaldehyde resin (PFR) nanocomposite for rapid, sensitive, and selective detection of glucose levels in human blood. In this biosensing system, MnO_2 nanoshell on the PFR nanoparticle surfaces serve as a quencher. PFR fluorescence can make a recovery in the presence of H_2O_2, reducing MnO_2 to Mn^{2+}. The sensor shows a linear range from 50 nM to 90 μM with a low detection limit of 20 nM for H_2O_2 detection. Thus, the glucose can be detected on the basis of the enzymatic conversion of glucose by glucose oxidase to produce H_2O_2. This method exhibits a wide linear range from 5 μM to 1 mM with a low detection limit of 1.5 μM. Because of the excellent photostability offered by PFR, the developed strategy has been successfully applied for the diagnosis of diabetes mellitus in human blood samples. Compared with commercial glucometer, our method showed satisfactory results, indicating the significant reliability. The developed turn-on fluorescent sensor might hold great promise in nanomedicine and bioanalysis.

Graphical abstract:

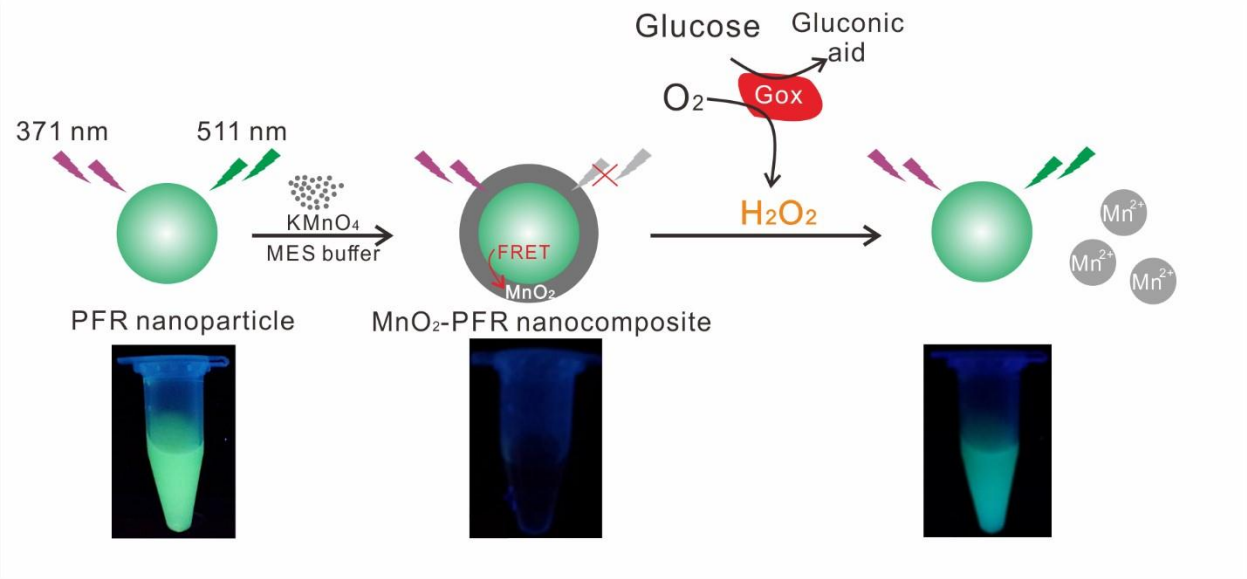

Keywords: phenol formaldehyde resin; manganese dioxide; glucose detection; fluorescent method; biosensor

1. Introduction

Diabetes mellitus (DM) is a major public metabolic disease that influences 366 million people in the world in 2011, and this number is predicted to rise to 552 million in 2030 [1,2]. DM is clinically diagnosed by a fasting blood glucose that equal or greater than 7 mM [3]. Therefore, the development of effective glucose biosensor has attracted extensive attention worldwide. Recently, various methods for the determination of glucose have been reported, such as colorimetry [4-8], fluorescence [9-13], electrochemistry [14-21], chemiluminescence [22,23], capillary electrophoresis [24], surface-enhanced Raman scattering [25], and surface plasmon resonance [26]. Among these noticeable methods, fluorescence-based strategies have sparked tremendous interest due to their rapid response, facile operation, and excellent sensitivity [27-30]. Many fluorescent compounds have been employed for precise analysis of glucose, including quantum dots [31,32], noble metal nanoclusters [33-35], up-converting nanoparticles [36-38], organic dyes [39-41], and composite fluorescent microspheres [42]. However, in many cases, the complicated material modification, intrinsic toxicity, and turn-off sensing mode cause inevitable disadvantages, including operational complexity, false results, and unsatisfactory sensitivity, for DM diagnosis [43,44]. Therefore, it remains a challenge to explore a simple, sensitive, and turn-on fluorescent method for reliable glucose detection and DM diagnosis.

Recently, Yu and co-workers has proposed a one-step hydrothermal synthetic approach of phenol formaldehyde resin (PFR) nanoparticle with the feature of superior photostability, excellent monodispersity, low cytotoxicity, and remarkable biocompatibility [45-47]. We previously discovered that MnO_2 can effectively quench the fluorescence of PFR by fluorescence resonance energy transfer (FRET) from PFR to MnO_2 and the fluorescence can be recovered by adding glutathione [48]. Since MnO_2-mediated quenching effect has been proved to reverse by

adding a small amount of H_2O_2 [37], we proposed a MnO_2-PFR nanocomposite for the selective and sensitive detection of glucose in blood on the basis of the enzymatic conversion of glucose by glucose oxidase (GOx) to generate H_2O_2. Our present MnO_2-PFR nanocomposite has several significant features compared with the previous glucose detection strategies: first, the MnO_2 decomposition technique offers turn-on fluorescent assay, which avoids the false result and improves the reliability of glucose detection in blood samples; second, PFR nanoparticles present remarkable photostability toward pH and ionic strength and accuracy compared with commercial glucometer, which ensure reliable signal output; third, because of the excellent accuracy, sensitivity, and selectively, the proposed sensing system can be employed for DM diagnosis (9 blood specimens from DM patients and 9 blood specimens from normal people were detected).

2. Material and methods

2.1 Materials

All reagents are of analytical grade and were used as received without any further purification. Potassium permanganate ($KMnO_4$), hydrogen peroxide (30% H_2O_2), phenol, sodium hydroxide (NaOH), 2-(N-morpholino)ethanesulfonic acid (MES), and glucose oxidase were obtained from Sigma Aldrich. Carbohydrate such as glucose, fructose, galactose, mannose and xylose used in this work were purchased from Aladdin Chemistry Co., Ltd. Hexamethylenetetramine (HMT) from Xiya Reagent. Blood specimens of normal and diabetic patient were obtained from Union Hospital, Tongji Medical College, Huazhong University of Science and Technology. Ultrapure water obtained from a Milli-Q ultrapure (18.2 MΩ) system was used throughout the experiment.

2.2 Instruments

The UV-Vis absorption spectra were recorded using Cary Eclipse UV-Vis Spectrophotometer (Agilent technologies). Fluorescence measurements were carried out by using Cary Eclipse fluorescence spectrophotometer (Agilent technologies). The morphology of nanoparticles was observed with a Tecnai G2 20 transmission electron microscopy (TEM) instrument with accelerating voltage of 200kV. The chemical composition and state were characterized by X-ray photoelectron spectroscopy (XPS) (Thermo Scientific Escalab 250XI). Dynamic light scattering (DLS) was conducted by Malvern Zetasizer Nano ZS (Malvern Instrument) to count the average size of the PFR and PFR-MnO_2 nanocomposite.

2.3 Synthesis of PFR nanoparticles

Our previous report was referred to synthesize PFR nanoparticles with some modifications [48]. The synthetic procedure was described as follows: 6.5 mg phenol and 5 mg HMT were dissolved in 50 mL of water. In the reaction, HMT was used as both the monomer (HCHO) source for polymerization and the cross-linking agent. After stirring intensely for 15 minutes, the solution was transferred into a Teflon lined autoclave and heated to 160 °C for 90 min. A solution with gray color was finally obtained. Then, the product was centrifuged and rinsed with ultrapure water and ethanol, respectively, to remove impurities for three times. The final product was redispersed in 10 mL of ultrapure water.

2.4 Synthesis of MnO_2-PFR nanocomposite

Fabrication of MnO_2-PFR nanocomposites were processed by mixing 1 mL of PFR (0.25 g/mL) nanoparticles with 2.5 mL of MES buffer (0.1M, pH 6.0). And then, 1 mL of $KMnO_4$ (10 mM) was added into it. After that, the resulting mixture was sonicated for 30 min until a brown colloid MnO_2-PFR nanocomposite was formed. MnO_2-PFR nanocomposite was centrifuged and

washed by ultrapure water for three times. The final product was redispersed in 10 mL of ultrapure water for subsequent reactions.

2.5 Fluorescence sensing of hydrogen peroxide

A 200 μL of MnO_2-PFR nanocomposite solution (0.1 g/mL) was mixed with 50 μL of a certain concentration of H_2O_2 at room temperature. After the incubation of a required reaction time, the mixture was transferred into a test quartz cuvette for fluorescence test. The emission fluorescence spectra were recorded at an excitation wavelength of 371 nm.

2.6 Fluorescence sensing of glucose

A 200 μL of MnO_2-PFR nanocomposite (0.1 g/mL) was mixed with 12.5 μL of a certain concentration of glucose and 37.5 μL of GOx for 15 min incubation at 37 °C. Afterward, the mixture was transferred to quartz cuvette for recording fluorescence emission spectra under 371 nm excitation. For the detection of glucose in practical samples, human whole blood specimens were centrifuged to obtain the serum for the detection.

3. Results and discussion

3.1 Working principle for H_2O_2 and glucose detection using MnO_2-PFR nanocomposite.

Based on the H_2O_2 modulation of MnO_2-induced fluorescent quenching of PFR nanoparticles, H_2O_2 and glucose detection strategy was designed (Scheme 1). To this end, PFR nanoparticles, the energy donors, with green fluorescence were synthesized by mixing phenol and HMT at 160 ℃ for 90 min (Scheme 1 A). The MnO_2 nanoshell were grow in situ and coated on the surface of PFR nanoparticles after a redox process of $KMnO_4$ in MES buffer under sonication treatment. Given the broad absorption band of MnO_2 from 300 to 450 nm [49], the green emission of PFR nanoparticles was significantly overlapped and the fluorescence of PFR nanoparticles was effectively quenched. By adding a small amount of H_2O_2, the MnO_2-induced

quenching effect can be reversed (Scheme 1 B). It might attribute to the H_2O_2-mediated reduction of MnO_2 to Mn^{2+}, resulting in the decomposition of MnO_2 accompanied by PFR fluorescence recovery. The reaction of MnO_2 to Mn^{2+} with addition of H_2O_2 is represented as eq 1 [37].

$$2H^+ + H_2O_2 + MnO_2 \rightarrow Mn^{2+} + O_2 + 2H_2O \quad (1)$$

Moreover, because H_2O_2 can be produced by oxidizing glucose in the presence of O_2 and GOx (eq 2) [13,21], a selective and sensitive turn on fluorescent assay can be realized for the blood glucose monitoring by detection of enzymatically generated H_2O_2.

$$\text{Glucose} + O_2 + H_2O \xrightarrow{\text{GOx}} \text{gluconic acid} + H_2O_2 \quad (2)$$

(Here Scheme 1)

3.2 Preparation and characterization of MnO_2-PFR nanocomposite

PFR nanoparticles were prepared with high water-dispersible property due to the hydroxyl and amino group on the surface of PFR [46]. MnO_2 nanoshell grew on the surface of the as-synthesized PFR by the addition of an aqueous $KMnO_4$ solution in the presence of MES buffer at pH 6. Thus, the MnO_2-PFR nanocomposite was formed. The morphologies of PFR nanoparticles, MnO_2-PFR nanocomposites with and without 300 μM H_2O_2 were characterized by TEM, respectively. Fig. 1A illustrated that PFR nanoparticles were spherical and well mono-dispersed, ranging from 19.2 to 34.3 nm and the average diameter is about 26.3 nm (Fig. S1A). Fig. 1B showed core-shell structure of MnO_2-PFR nanocomposite. The diameter significantly increased compared with mono-dispersed PFR nanoparticles. By DLS characterization, the size of MnO_2-PFR nanocomposite ranged from 458.7 to 825.0 nm with an average diameter of 637 nm (Fig. S1B), which was obviously larger than that of the unsheathed PFR. After the addition

of H_2O_2, the MnO_2 nanoshell was decomposed (Fig. 1C), releasing the mono-dispersed spherical PFR with an average diameter of 28.4 nm (Fig. S1C).

(Here Fig. 1)

To further characterize the deposition of MnO_2 on the surface of PFR, XPS spectroscopy analyses were employed**.** Fig. S2 depicted XPS results of PFR and MnO_2-PFR nanocomposite. It can be observed that the spectroscopy of PFR and MnO_2-PFR nanocomposite showed the existence of carbon (C1s, 284.82 eV), nitrogen (N1s, 399.71 eV), oxygen (O1s, 532.27 eV). Compared to PFR, the presence of the peak at 641.08eV was observed in the spectra of the MnO_2-PFR nanocomposite, which was ascribed to Mn 2p and the presence of Mn^{2+} [45-48]. These results verified the successful preparation of MnO_2-PFR nanocomposite assemblies.

The optical properties of PFR and MnO_2 were furtherly investigated. Fig. 2 showed the normalized UV–vis absorption of MnO_2 and normalized fluorescence emission spectra of PFR. The UV-vis spectrum of PFR exhibited a high and wide absorption band from 300 to 450 nm, which matched well with the previous published optical characteristics of MnO_2 nanomaterials [37,49]. Under the excitation at 371 nm, the PFR exhibits a bright green emission at 511 nm. The UV absorption of MnO_2 exhibited a remarkable spectral overlap with the green emissions of the PFR, enabling FRET process.

(Here Fig. 2)

The photostability of PFR toward complex ambient environments, such as high ionic strengths or extreme pH, plays a critical role in real-setting detection. Fig. S3 showed the fluorescence intensities of PFR at different pH values. As is shown, the PFR presented strong fluorescence activities in a wide pH range of 3–11, implying the excellent photostability under extreme pH conditions. Next, we studied the influence of ionic strengths on the photostability of

PFR in different concentrations of NaCl. As is shown in Fig. S4, the fluorescence intensity of PFR kept almost constant with increasing ionic strength from 0 to 1 M. The significant photostability might attribute to the unique chemical structure that no highly ionized functional groups presented on the PFR surface. Moreover, we found the fluorescence intensity of PFR slightly decreased even after 8 months (Fig. S5), which indicated the excellent photostability of PFR. Taking together, we might conclude the PFR possess significant photostability even under extreme conditions.

Since $KMnO_4$ was reduced to form MnO_2 nanoshell on the PFR surface in the presence of MES, the quenching efficiency of the $KMnO_4$ concentration was investigated in a fixed MES buffer. A series of MnO_2-PFR nanocomposites were prepared by changing $KMnO_4$ concentrations (from 0 to 10 mM). The fluorescence intensity of MnO_2-PFR nanocomposites decreased gradually with increasing $KMnO_4$ concentrations (Fig. S6A). Compared with the emission spectrum of fluorescent PFR nanoparticles without MnO_2 deposition, remarkable quenching at 511 nm was observed when 8 mM $KMnO_4$ was added. The effect of the $KMnO_4$ concentration on the quenching efficiency was displayed in Fig. S6B. The quenching efficiency was observed to gradually enhance with increasing the $KMnO_4$ concentration and it finally achieved a maximum value of ~73% when 8 mM $KMnO_4$ was presented. As a result, 8 mM $KMnO_4$ was chosen for subsequent experiments.

3.3 Detection of H_2O_2 based on the MnO_2–PFR nanocomposite

Having successfully prepared the MnO_2-PFR nanocomposite, the feasibility of H_2O_2 detection was then explored. We first verified the reduction of MnO_2 to Mn^{2+} in the presence of H_2O_2 by a highly specific reaction for Mn^{2+} as following equation [37]:

$$2Mn^{2+} + 5IO_4^- + 3H_2O \rightarrow 2MnO_4^- + 5IO_3^- + 6H^+ \quad (3)$$

The UV−vis absorption spectra of the MnO_2-PFR nanocomposite with H_2O_2 matched well with that of $KMnO_4$ solution from 400 to 700 nm, which demonstrated the presence of Mn^{2+} after the reaction of MnO_2-PFR nanocomposite with H_2O_2 (Fig. S7). Next, we investigated the fluorescence response of the MnO_2-PFR nanocomposite with the addition of H_2O_2. Although the fluorescence intensity was highly quenched, a significant fluorescence recovery (~90.8%) was observed after the addition of 300 μM H_2O_2 (Fig. 3A). Fig. 3B vividly showed the fluorescence quench and recovery process under the UV light. Then, we studied the dynamic response of fluorescence recovery. The time-dependent recovery showed the reaction of 300 μM H_2O_2 with the MnO_2-PFR nanocomposite reached to equilibrium rapidly in less than 5 minutes (Fig. S8), which is in favor of rapid practical applications.

(Here Fig. 3)

We next evaluated the response of the MnO_2-PFR nanocomposite at different H_2O_2 concentrations. The fluorescence was gradually recovered with increasing H_2O_2 concentration from 50 nM to 300 μM (Fig. 4A). The addition of 100 μM H_2O_2 caused a remarkable fluorescence signal recovery, which implied an almost complete recovery compared with that of PFR without MnO_2 modification. The fluorescence recovery of PFR is associated with the H_2O_2-mediated reduction of MnO_2 to Mn^{2+}, leading to the decomposition of MnO_2 nanoshell. Fig. 4B depicted the PFR fluorescence intensity at 511 nm as a function of the H_2O_2 concentration. The fluorescence intensity at 511 nm was linearly correlated with the H_2O_2 concentration in the range from 50 nM to 90 μM with a R^2 of 0.989 (Inset Fig.4B). The calibration equation is $y = 1.11\ x + 68.2$. The detection limit (3σ/slope, where σ is the standard deviation of the blank samples) was calculated to be 20 nM. Since the proposed turn-on fluorescent sensor has a good response toward H_2O_2 and glucose can be oxidized to generate H_2O_2 by GOx-catalyzed reaction, we

assume that the design of glucose detection based on the turn-on fluorescence of MnO_2-PFR nanocomposite is enabled.

(Here Fig. 4)

3.4 Detection of glucose based on MnO_2−PFR nanocomposite

Considering the significant importance of the blood glucose for the DM diagnosis, we further investigated the feasibility of MnO_2−PFR nanocomposite for glucose detection. We first investigated the effect of the incubation time on the fluorescence recovery response after glucose added (Fig. S9). When the incubation time was less than 15 min, the fluorescence intensity increased dramatically with increasing the incubation time. After 15 min, the fluorescence intensity reached equilibrium. Thus, the incubation time of 15 min were selected for glucose detection in terms of the best signal-to-background ratio. In addition, the GOx concentration was optimized (Fig. S10). The fluorescence intensity increased sharply with the increase of GOx concentration and it reached equilibrium at 0.64 mg mL^{-1}. Therefore, 0.64 mg mL^{-1} GOx was chose for the subsequent reaction.

We investigated the sensitivity of the turn-on fluorescent sensor to verify its potential to being a fast and simple protocol to detect glucose (Fig. 5A). The fluorescence intensity of the MnO_2-PFR nanocomposite at 511 nm increases gradually upon increasing the concentration of glucose from 5 μM to 20 mM. As shown in Fig. 5B, the calibration equation serves as the quantitative basis for the fluorescence intensity enhancement against the concentration of glucose. The fluorescence intensity increased almost linearly with increasing glucose concentration, varying from 5 μM to 1 mM. The regression equation is $y = 68.3\ x + 71.6$ with a R^2 of 0.991. The detection limit of glucose was calculated to be 1.5 μM (3σ/slope). The detection limit obtained from this method was found to be better than the other methods listed in Table S1.

(Here Fig. 5)

The capability of distinguishing the target molecule from the interferences normally present in a complex biological environment, which is extremely important for a sensor**.** Therefore, the selectivity of the proposed biosensor was gauged with some analogs, such as fructose, galactose, mannose, xylose, and arabinose. Fig. 5C displayed selectivity results of the method toward glucose in the presence of other interfering species. Significant signal change was observed when glucose added and other interfering species barely influent the fluorescence intensity, revealing the remarkable selectivity of this approach toward glucose over other tested carbohydrates.

To evaluate the feasibility of the MnO_2-PFR nanocomposite for glucose detection in complex biological samples, the proposed strategy was applied for the diagnosis of DM by detecting 18 clinically whole blood samples, including 9 normal people specimens and 9 DM specimens. Whole blood samples were centrifuged to obtain the serum before detection process. Consideration the normal glucose level in healthy human blood and the linear range of this method, 12.5 μL of specimens was added to the reaction system and diluted to 250 μL for the detection, which was a 20-fold dilution. After the GOx-catalyzed reaction to the clinically specimens, the fluorescence intensity of MnO_2-PFR nanocomposite in DM specimens increased obviously. However, the normal specimens presented a low fluorescence intensity (Fig. 5D). The calculated glucose concentrations of the DM and normal specimens were within the range of 11.3−19.2 mM and 4.7−6.2 mM (Table S2), which are close to the results that measured by commercial glucometer. Satisfactory recoveries of glucose from DM specimens were obtained (95.6%-106.1%) with a relative standard deviation (RSD) from 2.9% to 6.8%, and glucose

recoveries from normal specimens (92.3%-105.7%) were achieved with a RSD from 2.1% to 6.8%, indicating the excellent accuracy and reliability of this method.

4. Conclusions

We have demonstrated a novel strategy based on MnO_2-PFR nanocomposite for rapid monitoring of blood glucose levels. Combining the sensitive MnO_2-H_2O_2 reaction with the fluorescent advantage of PFR nanoparticles, a highly selective, sensitive, and rapid sensing method for glucose detection has been developed and applied to monitor glucose levels in human blood samples with satisfactory results. Compared with the commercial glucometer, our sensor displayed excellent reliability. The proposed biosensing system is promising for diabetes mellitus diagnosis and clinical research. In addition, this biosensing system is generalizable and might be extended easily for the detection of various H_2O_2-involved targets. The proposed approach might provide a new insight to develop sensitive and reliable methods for biological and clinical diagnostics applications.

Acknowledgements

This work is supported by National Basic Research Program of China (973 Program, 2015CB932600, 2013CB933000, 2016YFF0100800), the National Natural Science Foundation of China (21375042, 21405054, 21525523, 21574048), China Postdoctoral Science Foundation (2016M602276), and 1000 Young Talent (to F.X.).

Appendix A. Supplementary information

Supplementary data associated with this article can be found, in the online version, at doi:10.1016/j.bios.201X.XX.XXX.

References

[1] H. Li, C. Liu, D. Wang, C. Zhang, Chemiluminescence cloth-based glucose test sensors (CCGTSs): A new class of chemiluminescence glucose sensors, Biosens. Bioelectron. 91 (2017) 268–275.

[2] J.L. Ma, B.C. Yin, X. Wu, B.C. Ye, Simple and cost-effective glucose detection based on carbon nanodots supported on silver nanoparticles, Anal. Chem. 89 (2017) 1323–1328.

[3] S.P. Nichols, A. Koh, W.L. Storm, J.H. Shin, M.H. Schoenfisch, Biocompatible materials for continuous glucose monitoring devices, Chem. Rev. 113 (2013) 2528–2549.

[4] L. Lin, X. Song, Y. Chen, M. Rong, T. Zhao, Y. Wang, Y. Jiang, X. Chen, Intrinsic peroxidase-like catalytic activity of nitrogen-doped graphene quantum dots and their application in the colorimetric detection of H_2O_2 and glucose, Anal. Chim. Acta. 869 (2015) 89–95.

[5] A.K. Dutta, S. Das, S. Samanta, P.K. Samanta, B. Adhikary, P. Biswas, CuS nanoparticles as a mimic peroxidase for colorimetric estimation of human blood glucose level, Talanta 107 (2013) 361–367.

[6] C. Lu, X. Liu, Y. Li, F. Yu, L. Tang, Y. Hu, Y. Ying, Multifunctional Janus hematite-silica nanoparticles: mimicking peroxidase-like activity and sensitive colorimetric detection of glucose, ACS Appl. Mater. Interfaces. 7 (2015) 15395–15402.

[7] L. Su, J. Feng, X. Zhou, C. Ren, H. Li, X. Chen, Colorimetric detection of urine glucose based $ZnFe_2O_4$ magnetic nanoparticles, Anal. Chem. 84 (2012) 5753–5758.

[8] G.L. Wang, X. Xu, X. Wu, G. Cao, Y. Dong, Z. Li, Visible-light-stimulated enzymelike activity of graphene oxide and its application for facile glucose sensing, J. Phys. Chem. C. 118 (2014) 28109–28117.

[9] Z. Liu, L. Liu, M. Sun, X. Su, A novel and convenient near-infrared fluorescence "turn off-on" nanosensor for detection of glucose and fluoride anions, Biosens. Bioelectron. 65 (2015) 145–151.

[10] V.V. Karnati, X. Gao, S. Gao, W. Yang, W. Ni, S. Sankar, B. Wang, A glucose-selective fluorescence sensor based on boronic acid-diol recognition, Bioorg. Med. Chem. Lett. 12 (2002) 3373–3377.

[11] F. Hu, Y. Huang, G. Zhang, R. Zhao, D. Zhang, A highly selective fluorescence turn-on detection of hydrogen peroxide and d-glucose based on the aggregation/deaggregation of a modified tetraphenylethylene, Tetrahedron Lett. 55 (2014) 1471–1474.

[12] Y.S. Li, Y.D. Du, T.M. Chen, X.F. Gao, A novel immobilization multienzyme glucose fluorescence capillary biosensor, Biosens. Bioelectron. 25 (2010) 1382–1388.

[13] Y. Ling, N. Zhang, F. Qu, T. Wen, Z.F. Gao, N.B. Li, H.Q. Luo, Fluorescent detection of hydrogen peroxide and glucose with polyethyleneimine-templated Cu nanoclusters, Spectrochim. Acta - Part A 118 (2014) 315–320.

[14] Y.S. Ko, Y.U. Kwon, Mesoporous zirconia thin films with three-dimensional pore structures and their application to electrochemical glucose detection, ACS Appl. Mater. Interfaces. 5 (2013) 3599–606.

[15] X. Jia, G. Hu, F. Nitze, H.R. Barzegar, T. Sharifi, C.W. Tai, T. Wagberg, Synthesis of palladium/helical carbon nanofiber hybrid nanostructures and their application for hydrogen peroxide and glucose detection, ACS Appl. Mater. Interfaces. 5 (2013) 12017–12022.

[16] C.M. Zook, W.R. LaCourse, Pulsed amperometric detection of microdialysates from the glucose oxidase reaction, Anal. Chem. 70 (1998) 801–806.

[17] J. Noiphung, T. Songjaroen, W. Dungchai, C.S. Henry, O. Chailapakul, W. Laiwattanapaisal, Electrochemical detection of glucose from whole blood using paper-based microfluidic devices, Anal. Chim. Acta. 788 (2013) 39–45.

[18] W. Lu, Y. Sun, H. Dai, P. Ni, S. Jiang, Y. Wang, Z. Li, Z. Li, Direct growth of pod-like Cu_2O nanowire arrays on copper foam: Highly sensitive and efficient nonenzymatic glucose and H_2O_2 biosensor, Sens. Actuators B 231 (2016) 860–866.

[19] S. Su, H. Sun, F. Xu, L. Yuwen, C. Fan, L. Wang, Direct electrochemistry of glucose oxidase and a biosensor for glucose based on a glass carbon electrode modified with MoS_2 nanosheets decorated with gold nanoparticles, Microchim. Acta. 181 (2014) 1497–1503.

[20] B.U. Moon, S. Koster, K.J.C. Wientjes, R.M. Kwapiszewski, A.J.M. Schoonen, B.H.C. Westerink, E. Verpoorte, An enzymatic microreactor based on chaotic micromixing for enhanced amperometric detection in a continuous glucose monitoring application, Anal. Chem. 82 (2010) 6756–6763.

[21] Z.F. Gao, D.M. Chen, J.L. Lei, H.Q. Luo, N.B. Li, A regenerated electrochemical biosensor for label-free detection of glucose and urea based on conformational switch of i-motif oligonucleotide probe, Anal. Chim. Acta. 897 (2015) 10–16.

[22] T.Y. Yeh, C.I. Wang, H.T. Chang, Photoluminescent C-dots@RGO for sensitive detection of hydrogen peroxide and glucose, Talanta 115 (2013) 718–723.

[23] N. Li, W. Diao, Y. Han, W. Pan, T. Zhang, B. Tang, MnO_2-modified persistent luminescence nanoparticles for detection and imaging of glutathione in living cells and in vivo, Chem. Eur. J. 20 (2014) 16488–16491.

[24] X. Wang, Y. Ma, M. Zhao, M. Zhou, Y. Xiao, Z. Sun, L. Tong, Determination of glucose in human stomach cancer cell extracts and single cells by capillary electrophoresis with a micro-biosensor, J. Chromatogr. A 1469 (2016) 128–134.

[25] K.E. Shafer-Peltier, C.L. Haynes, M.R. Glucksberg, R.P. Van Duyne, Toward a glucose biosensor based on surface-enhanced Raman scattering, J. Amer. Chem. Soc. 125 (2003) 588–593.

[26] L. Tian, J. Qiu, Y.C. Zhou, S.G. Sun, Application of polypyrrole/GOx film to glucose biosensor based on electrochemical-surface plasmon resonance technique, Microchim. Acta. 169 (2010) 269–275.

[27] M. Hu, J. Tian, H.T. Lu, L.X. Weng, L.H. Wang, H_2O_2-sensitive quantum dots for the label-free detection of glucose, Talanta 82 (2010) 997–1002.

[28] L. Jin, L. Shang, S. Guo, Y. Fang, D. Wen, L. Wang, J. Yin, S. Dong, Biomolecule-stabilized Au nanoclusters as a fluorescence probe for sensitive detection of glucose, Biosens. Bioelectron. 26 (2011) 1965–1969.

[29] J.W. Liu, Y. Luo, Y.M. Wang, L.Y. Duan, J.H. Jiang, R.Q. Yu, Graphitic carbon nitride nanosheets-based ratiometric fluorescent probe for highly sensitive detection of H_2O_2 and glucose, ACS Appl. Mater. Interfaces. 8 (2016) 33439–33445.

[30] H. Zhai, T. Feng, L. Dong, L. Wang, X. Wang, H. Liu, Y. Liu, L. Chen, M.X. Xie, Development of dual-emission ratiometric probe-based on fluorescent silica nanoparticle and CdTe quantum dots for determination of glucose in beverages and human body fluids, Food Chem. 204 (2016) 444–452.

[31] X. Shan, L. Chai, J. Ma, Z. Qian, J. Chen, H. Feng, B-doped carbon quantum dots as a sensitive fluorescence probe for hydrogen peroxide and glucose detection., Analyst 139 (2014) 2322–5.

[32] Z. Qu, X. Zhou, L. Gu, R. Lan, D. Sun, D. Yu, G. Shi, Boronic acid functionalized graphene quantum dots as a fluorescent probe for selective and sensitive glucose determination in microdialysate., Chem. Commun. 49 (2013) 9830–9832.

[33] L. Hu, Y. Yuan, L. Zhang, J. Zhao, S. Majeed, G. Xu, Copper nanoclusters as peroxidase mimetics and their applications to H_2O_2 and glucose detection, Anal. Chim. Acta. 762 (2013) 83–86.

[34] L.L. Wang, J. Qiao, H.H. Liu, J. Hao, L. Qi, X.P. Zhou, D. Li, Z.X. Nie, L.Q. Mao, Ratiometric fluorescent probe based on gold nanoclusters and alizarin red-boronic acid for monitoring glucose in brain microdialysate, Anal. Chem. 86 (2014) 9758–9764.

[35] X. Liu, F. Wang, A. Niazov-Elkan, W. Guo, I. Willner, Probing biocatalytic transformations with luminescent DNA/silver nanoclusters, Nano Lett. 13 (2013) 309–314.

[36] M.D Barrio, S.D Marcos, V. Cebolla, J. Heiland, S. Wilhelm, T. Hirsch, J. Galbán, Enzyme-induced modulation of the emission of upconverting nanoparticles: Towards a new sensing scheme for glucose, Biosens. Bioelectron. 59 (2014) 14–20.

[37] J. Yuan, Y. Cen, X.J. Kong, S. Wu, C.L. Liu, R.Q. Yu, X. Chu, MnO_2 nanosheet-modified upconversion nanosystem for sensitive turn-on fluorescence detection of H_2O_2 and glucose in blood, ACS Appl. Mater. Interfaces 7 (2015) 10548–10555.

[38] H. Chen, A. Fang, L. He, Y. Zhang, S. Yao, Sensitive fluorescent detection of H_2O_2 and glucose in human serum based on inner filter effect of squaric acid-iron(III) on the fluorescence of upconversion nanoparticle, Talanta 164 (2017) 580–587.

[39] J. Li, J. Chen, Y. Chen, Y. Li, S.A. Shahzad, Y. Wang, M. Yang, C. Yu, Fluorescence turn-on detection of mercury ions based on the controlled adsorption of a perylene probe onto the gold nanoparticles, Analyst 141 (2016) 346–351.

[40] B. Liu, Z. Sun, P.J.J. Huang, J. Liu, Hydrogen peroxide displacing DNA from nanoceria: Mechanism and detection of glucose in serum, J. Am. Chem. Soc. 137 (2015) 1290–1295.

[41] A.A. Essawy, M.S. Attia, Novel application of pyronin Y fluorophore as high sensitive optical sensor of glucose in human serum, Talanta 107 (2013) 18–24.

[42] Y. Li, Q. Ma, Z. Liu, X. Wang, X. Su, A novel enzyme-mimic nanosensor based on quantum dot-Au nanoparticle@silica mesoporous microsphere for the detection of glucose, Anal. Chim. Acta. 840 (2014) 68–74.

[43] Q. Ke, Y. Zheng, F. Yang, H. Zhang, X. Yang, A fluorescence glucose sensor based on pH induced conformational switch of i-motif DNA, Talanta 129 (2014) 539–544.

[44] H. Ma, X. Liu, X. Wang, X. Li, C. Yang, A. Iqbal, W. Liu, J. Li, W. Qin, Sensitive fluorescent light-up probe for enzymatic determination of glucose using carbon dots modified with MnO_2 nanosheets, Microchim. Acta. 184 (2017) 177–185.

[45] P. Yang, Y. Zhao, Y. Lu, Q.Z. Xu, X.W. Xu, L. Dong, S.H. Yu, Phenol formaldehyde resin nanoparticles loaded with CdTe quantum dots: A fluorescence resonance energy transfer probe for optical visual detection of copper (II) ions, ACS Nano 5 (2011) 2147–2154.

[46] B.S. Guo, J.Y. Gong, P. Jiang, M. Wu, Y. Lu, S.H. Yu, S.R. Guo, J.Y. Gong, P. Jiang, M. Wu, Y. Lu, S.H. Yu, Biocompatible, luminescent silver@phenol formaldehyde resin core/shell nanospheres: Large-scale synthesis and application for in vivo bioimaging, Adv. Funct. Mater. 18 (2008) 872–879.

[47] P. Yang, Q.Z. Xu, S.Y. Jin, Y. Zhao, Y. Lu, X.W. Xu, S.H. Yu, Synthesis of Fe_3O_4 @ phenol formaldehyde resin core – shell nanospheres loaded with Au nanoparticles as magnetic FRET nanoprobes for detection of thiols in living cells, Chem. Eur. J. 18 (2012) 1154–1160.

[48] X. Wang, D. Wang, Y. Guo, C. Yang, X. Liu, A. Iqbal, W. Liu, W. Qin, D. Yan, H. Guo, Fluorescent glutathione probe based on MnO_2-phenol formaldehyde resin nanocomposite, Biosens. Bioelectron. 77 (2016) 299–305.

[49] X.L. Zhang, C. Zheng, S.S. Guo, J. Li, H.H. Yang, G. Chen, Turn-on fluorescence sensor for intracellular imaging of glutathione using g-C_3N_4 nanosheet-MnO_2 sandwich nanocomposite. Anal. Chem. 86 (2014), 3426−3434.

Figure captions:

Scheme 1. Schematic representation of (A) preparation of PFR nanoparticles and (B) glucose sensor by turn-on fluorescence of the MnO_2-PFR nanocomposite.

Figure 1. TEM image of (A) PFR nanoparticles, (B) MnO_2-PFR nanocomposite, (C) MnO_2-PFR nanocomposite with 300 μM H_2O_2.

Figure 2. Normalized UV-Vis absorption spectra of aqueous solutions of MnO_2 nanosheets (green curve) and normalized fluorescence spectra (red curve) of PFR nanoparticles.

Figure 3. (A) Fluorescence emission spectra of PFR nanoparticles (curve a), MnO_2-PFR nanocomposite in the absence (curve b) and presence (curve c) of 300 μM H_2O_2. (B) Photographic fluorescence response of (a) PFR nanoparticles, (b) MnO_2-PFR nanocomposite, and (c) recovered fluorescent PFR nanoparticles after 300 μM H_2O_2 added under UV light (excited at 365 nm).

Figure 4. (A) Fluorescence emission spectra of MnO_2-PFR nanocomposite in the presence of different concentrations of H_2O_2 (a-k: 50 nM, 100 nM, 5 μM, 10 μM, 20 μM, 30 μM, 50 μM, 70 μM, 90 μM, 150 μM, and 300 μM, respectively). (B) The corresponding calibration plot for H_2O_2 detection. The inset was the enlarged linear plot of the fluorescence intensity against the H_2O_2 concentration. Error bars indicate the standard deviation of three replicates.

Figure 5. (A) Fluorescence emission spectra of MnO_2-PFR nanocomposite in the presence of different concentrations of glucose (a-n: 5 μM, 10 μM, 100 μM, 200 μM, 400 μM, 600 μM, 800 μM, 1 mM, 3 mM, 5 mM, 6 mM, 8 mM, 10 mM, and 20 mM, respectively). (B) The corresponding calibration plot for glucose detection. Inset shows the enlarged linear relationship

between fluorescence intensity and values of glucose concentration. (C) Selectivity of the method towards glucose sensing in the presence of other interfering species. The concentrations of all the saccharides kept constant 5 mM. (D) Results of the MnO_2-PFR nanocomposite for the diagnosis of DM in real blood specimens. Error bars indicate the standard deviation of three replicates.

Scheme 1.

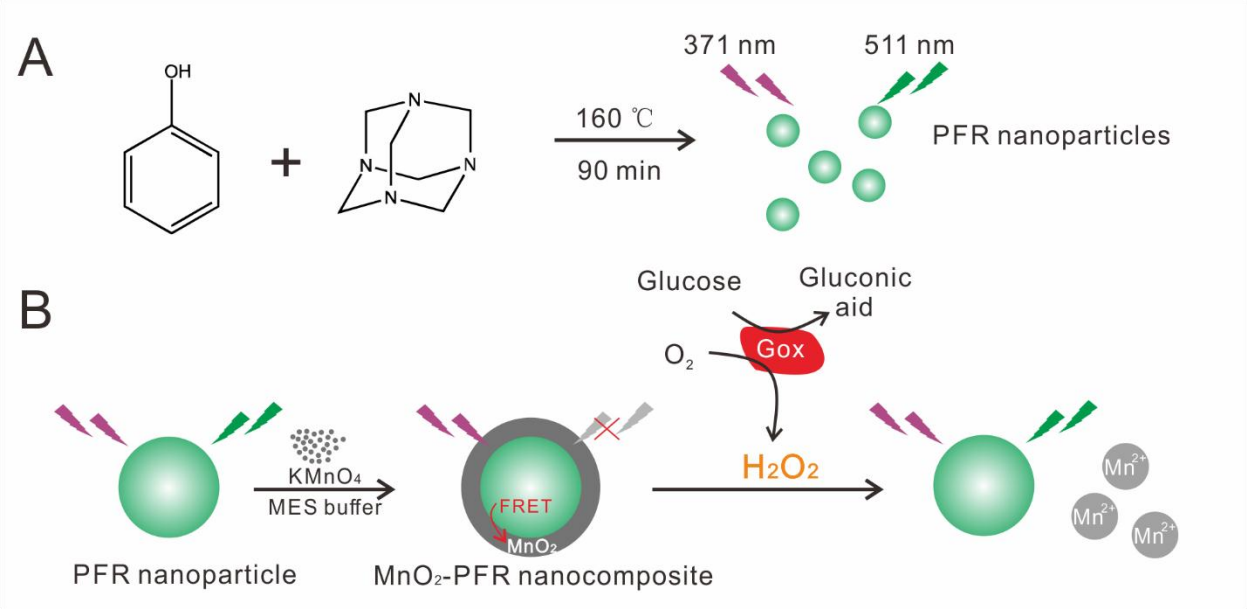

Fig. 1

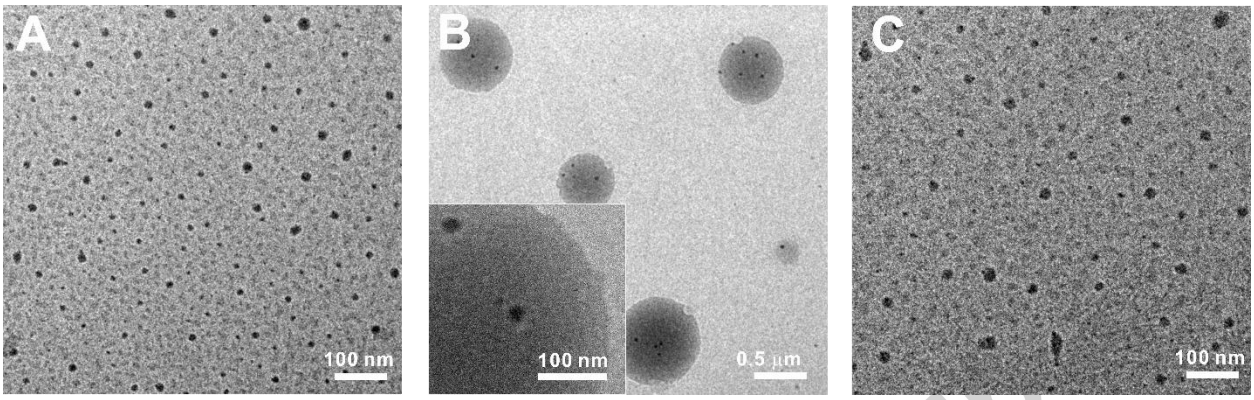

Fig. 2

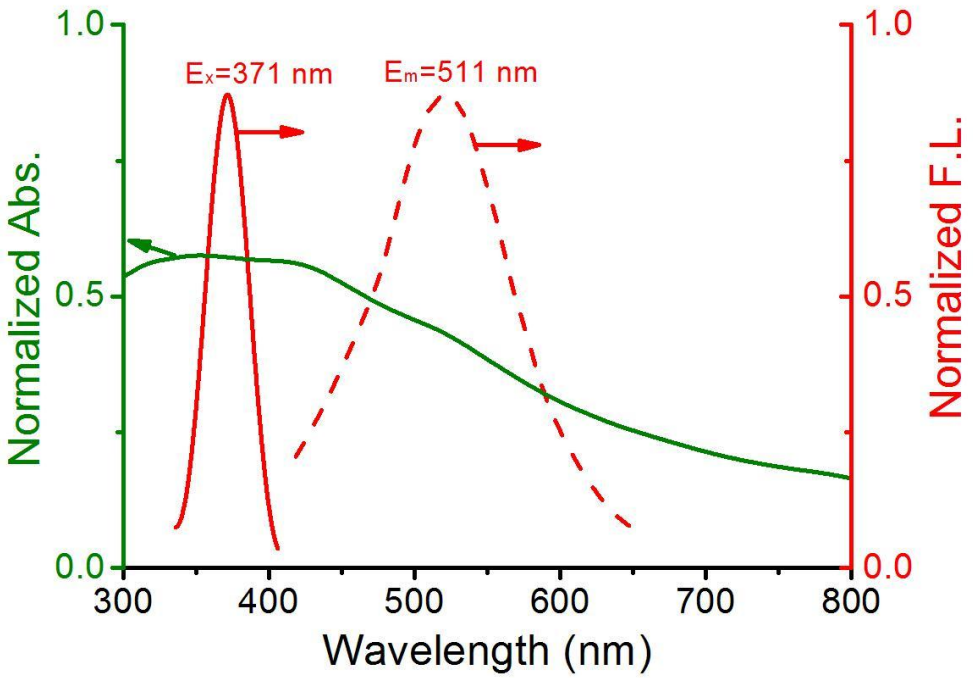

Fig. 3

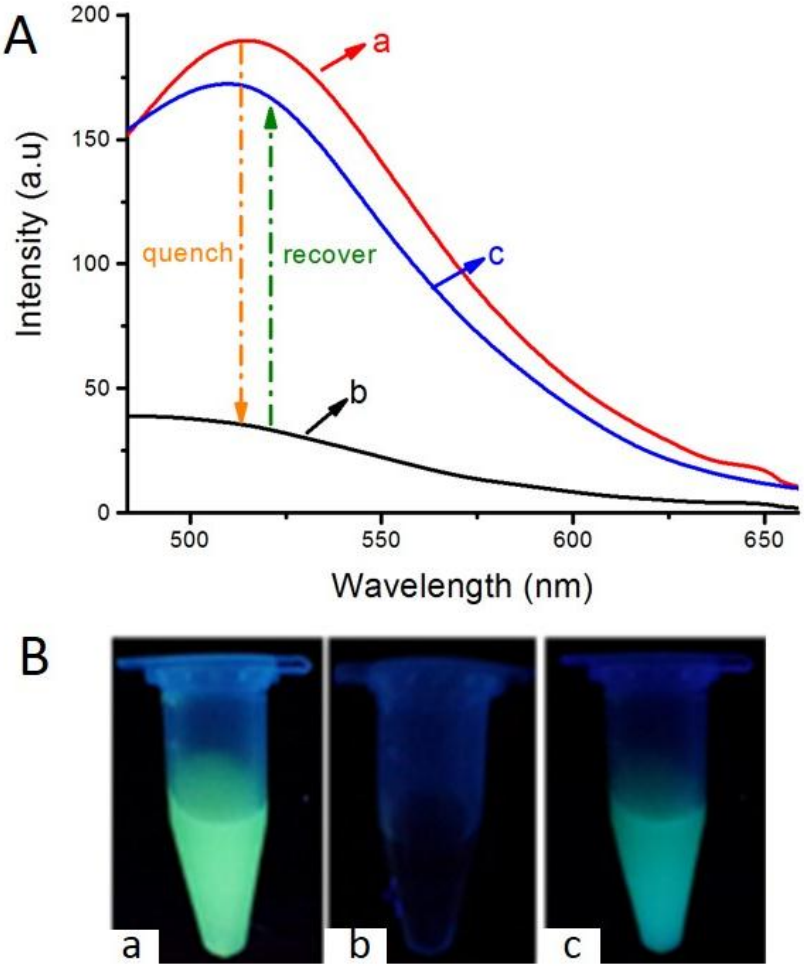
A
200
150
100
50
0
Intensity (a.u)
a
b
c
quench
recover
500
550
600
650
Wavelength (nm)
B
a
b
c

Fig. 4

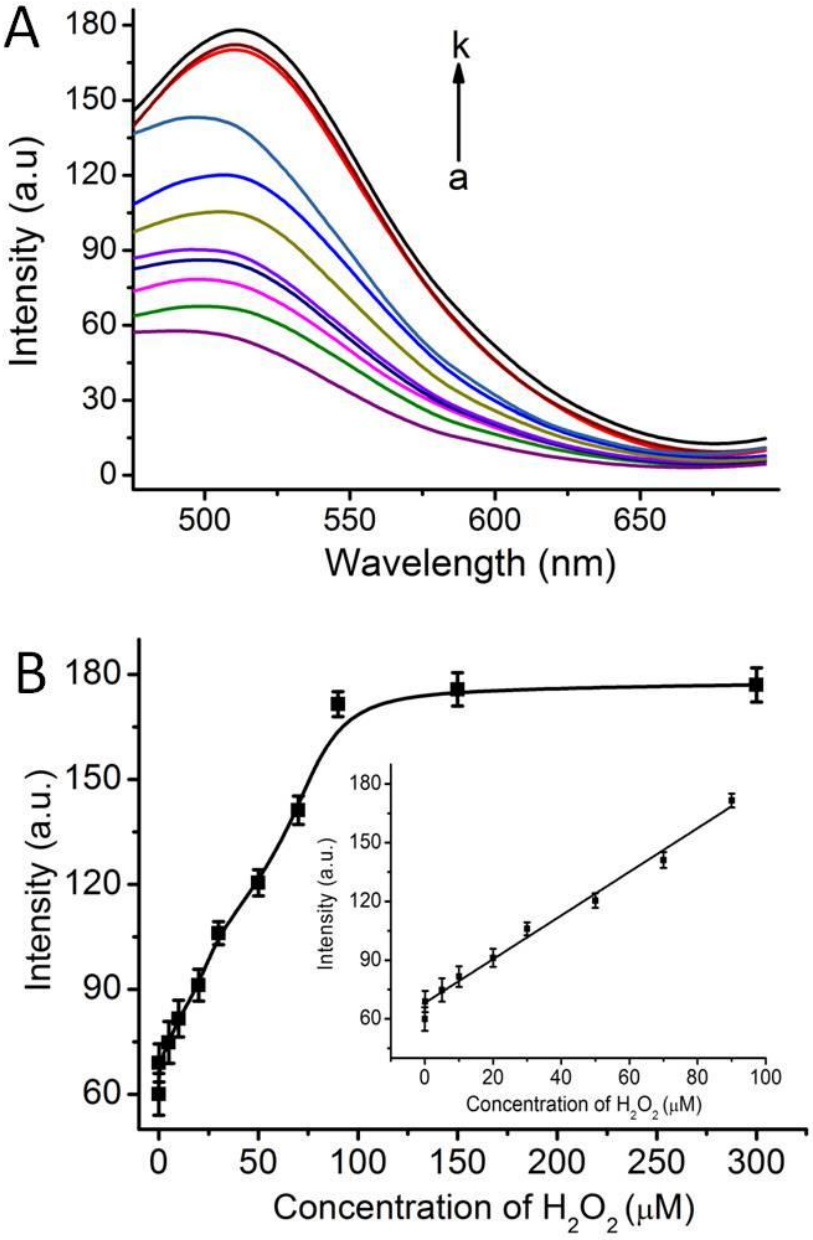
A
Intensity (a.u)
Wavelength (nm)
k
a
B
Intensity (a.u.)
Concentration of H_2O_2 (μM)
Intensity (a.u.)
Concentration of H_2O_2 (μM)

Fig. 5

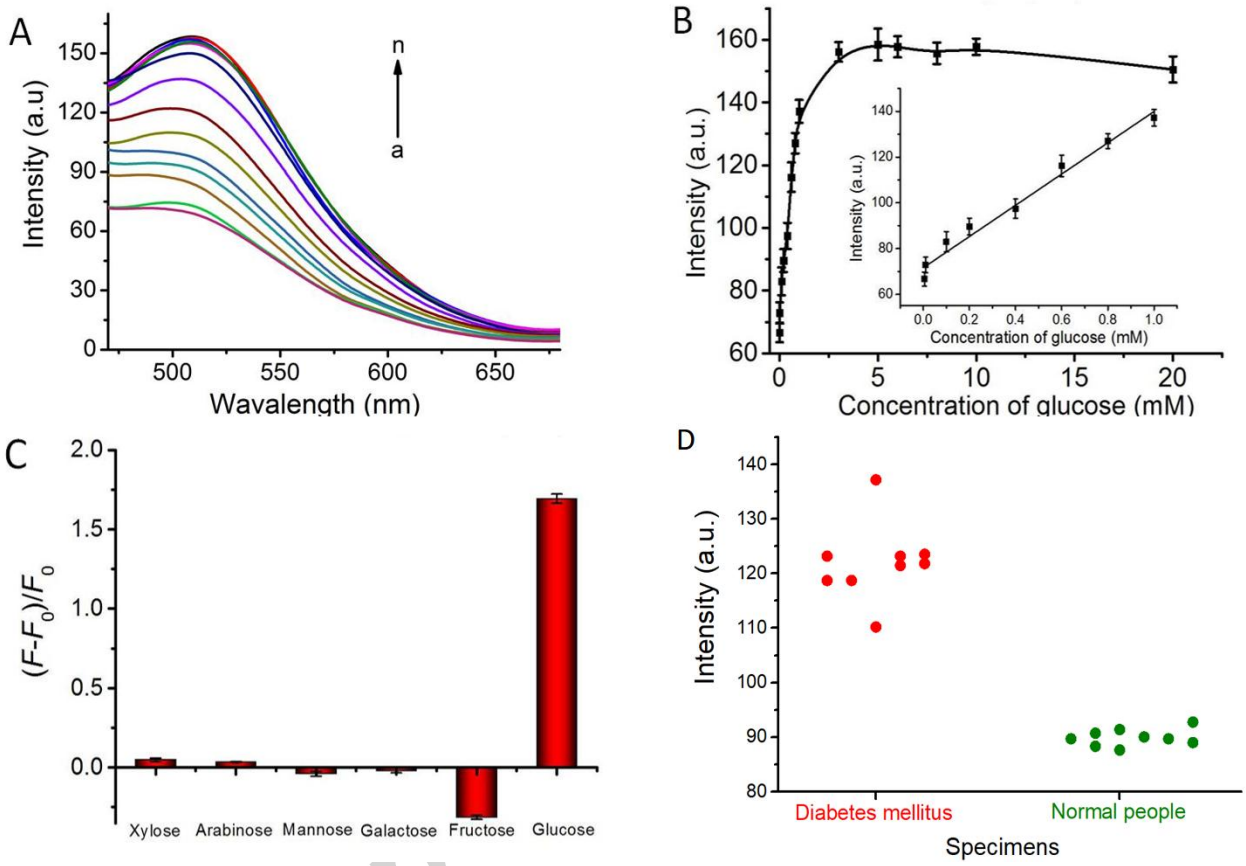

Highlights

- The MnO_2-PFR nanocomposite was successfully synthesized.
- The fluorescence of PFR can be recovered by H_2O_2 due to reduction of MnO_2 to Mn^{2+}.
- The proposed method is applied for diabetes mellitus diagnosis.
- The method is reliable compared with commercial glucometer.